JOURNAL OF GEOPHYSICAL RESEARCH, VOL. 114, A00C09, doi:10.1029/2008JA013559, 2009

Timing and localization of ionospheric signatures associated with substorm expansion phase onset

I. Jonathan Rae,[1] Ian R. Mann,[1] Kyle R. Murphy,[1] David K. Milling,[1] Adrienne Parent,[1] Vassilis Angelopoulos,[2] Harald U. Frey,[3] Andy Kale,[1] Clare E. J. Watt,[1] Stephen B. Mende,[3] and Christopher T. Russell[2]

Received 2 July 2008; revised 28 August 2008; accepted 14 October 2008; published 22 January 2009.

[1] In this paper, we present case studies of the optical and magnetic signatures of the characteristics of the first minute of substorm expansion phase onset observed in the ionosphere. We find that for two isolated substorms, the onset of magnetic pulsations in the 24–96 s period wavelet band are colocated in time and space with the formation and development of small-scale optical undulations along the most equatorward preexisting auroral arc prior to auroral breakup. These undulations undergo an inverse spatial cascade into vortices prior to the release of the westward traveling surge. We also present a case study of a multiple activation substorm, whereby discrete onsets of ULF wave power above a predetermined quiet time threshold are shown to be associated with specific optical intensifications and brightenings. Moreover, in the multiple activation substorm event, we show that neither the formation of the small-scale undulations nor the formation of similar structures along a north–south aligned arc is sufficient to produce auroral breakup associated with expansion phase onset. It is only ~10 min after these two disparate activation regions initiate that auroral breakup and the subsequent formation of a westward traveling surge occur. We discuss the implications of these results in terms of the triggering mechanisms likely to be occurring during these specific events.

Citation: Rae, I. J., et al. (2009), Timing and localization of ionospheric signatures associated with substorm expansion phase onset *J. Geophys. Res.*, *114*, A00C09, doi:10.1029/2008JA013559.

1. Introduction

[2] The physics surrounding substorm onset has been a topic of considerable date for over 40 years [*Akasofu*, 1964]. A large part of the controversy surrounds the question of whether current disruption (CD) via plasma instabilities in the near-Earth plasma sheet are responsible for substorm expansion phase onset (at distances $\leq$12 R_E in the magnetotail [e.g., *Roux et al.*, 1991; *Lui.*, 1991]), or whether the near-Earth disturbances require prior bursts of magnetic reconnection at a near-Earth neutral line (NENL) in the midtail which trigger substorm onset (at ~20–30 R_E [*Hones et al.*, 1970a, 1970b; *Nagai et al.*, 1998]). Central to answering this question is the ability to time and monitor the location of substorm expansion phase onset both in the magnetosphere and ionosphere. Determining the location of substorm onset in the ionosphere both optically and magnetically is therefore a fundamental aspect of substorm physics, and is crucial for resolving the causal sequence of events surrounding onset.

[3] Historically, substorm expansion phase onsets are identified optically by the brightening of a preexisting quiet discrete arc usually in the midnight sector, or in some cases by the formation of a new discrete arc [*Akasofu*, 1964, 1977]. Magnetically, this is accompanied by Pi2 (40–150 s [*Jacobs et al.*, 1964]) pulsations observed on the ground that "ride" on magnetic bay structures, believed to develop when the cross-tail current is diverted toward the ionosphere as the nightside magnetic field dipolarizes, forming the Substorm Current Wedge (SCW) [e.g., *Atkinson*, 1967; *McPherron et al.*, 1973]. The polarization of Pi2s may be used to identify the location of the SCW [e.g., *Lester et al.*, 1983], defining the upward and downward field-aligned current (FAC) element meridians, and hence an estimate of the location of the central meridian. However, it is evident that the "2-minute problem" surrounding expansion phase onset [*Ohtani*, 2004] cannot be resolved using Pi2 pulsations since their wave period is ~1–2 min. Similarly, Pi2s tend to have global characteristics in the ionosphere such that they cannot be used to determine the ionospheric onset location [e.g., *Yumoto et al.*, 1990]. However, shorter period ULF wave bands such as those in the Pi1B (1–10 s) part of the Pi1 band (1–40 s [*Jacobs et al.*, 1964]) have been shown to be able to reduce this uncertainty [e.g., *Bösinger*, 1989; *Lessard et al.*, 2006] but only in a localized region

[1]Department of Physics, University of Alberta, Edmonton, Alberta, Canada.
[2]Institute of Geophysics and Planetary Physics, University of California, Los Angeles, California, USA.
[3]Space Sciences Laboratory, University of California, Berkeley, California, USA.

0148-0227/09/2008JA013559$09.00

close to onset [e.g., *Bösinger and Yahnin*, 1987; *Arnoldy et al.*, 1987; *Bösinger*, 1989]. Thus, Pi1B-onset determination requires favorable conditions to be present during onset. *Posch et al.* [2007] found that there was a significant drop off of Pi1B amplitude (as a function of distance cubed) away from the ionospheric location of substorm onset.

[4] Recently, ULF waves in the longer-period Pi1 band were used by *Milling et al.* [2008] to diagnose the timing and localized ULF wave onset location in the ionosphere using a discrete wavelet technique (DWT) using a Meyer wavelet basis (compare to the Pi2 timing described by *Nose et al.* [1998]). In their paper, *Milling et al.* [2008] showed that the onset of 12–48 s period ULF waves had a clear and coherent onset pattern that spread out from an epicenter. Their study presented the first evidence that the longer-period Pi1 waves may be able to provide crucial information about the characteristics during the first tens of seconds of expansion phase onset in the ionosphere. During substorms, Pi2 pulsations are observed simultaneously over a large ionospheric region, and Pi1B pulsations require a station closely conjugate to the onset location to be readily observable. As a result, neither of these ULF wave bands are routinely available for substorm onset diagnosis. The long-period Pi1 ULF wave band may offer a compromise between these two ULF band extremes.

[5] Recently, a new auroral feature associated with expansion phase onset has also been receiving attention [e.g., *Donovan et al.*, 2007; *Liang et al.*, 2008; I. J. Rae et al., Near-Earth initiation of terrestrial substorm onset, submitted to *Journal of Geophysical Research*, 2008]. Using the THEMIS white light All-Sky Imagers (ASIs) [*Mende et al.*, 2008], these authors observed small-scale (~50–70 km) optical undulations with time scales of ~10 s which develop on the equatorwardmost discrete arc. These undulations were observed by Rae et al. (submitted manuscript, 2008) to grow and propagate along the arc for ~1 min prior to auroral breakup and ~3 min prior to the release of the westward traveling surge (WTS). During this time, preexisting discrete arcs poleward of the onset arc remained static on this time scale, suggesting the arc undulations are the ionospheric auroral signatures resulting from the development of an isolated near-Earth instability which does not perturb the more tailward plasma sheet and hence the higher-latitude preonset discrete arcs (Rae et al., submitted manuscript, 2008).

[6] The THEMIS mission [*Sibeck and Angelopoulos*, 2008; *Angelopoulos*, 2008] is designed to resolve the lack of ionospheric spatial coverage both optically with the THEMIS ASIs and magnetically with the THEMIS GMAGs [*Russell et al.*, 2008], while providing contemporaneous high-fidelity five point magnetically conjugate measurements in space during substorms [*Angelopoulos et al.*, 2008a, 2008b]. The THEMIS GMAG array includes data from five stations of the Canadian Array for Realtime Investigations of Magnetic Activity (CARISMA) [*Mann et al.*, 2008] array, and the GMAG monitoring is augmented by available data from additional stations in the CARISMA array and from stations in the Canadian Magnetic Observatory System (CANMOS) and Geophysical Institute Magnetometer Array (GIMA) arrays. Data from all of these magnetometer arrays are used in this study.

[7] Using the technique outlined by *Milling et al.* [2008] and presented in detail by *Murphy et al.* [2008], we build on the result outlined by Rae et al. (submitted manuscript, 2008) which demonstrated that the ionospheric Pi1 ULF wave onset is contemporaneous and colocated with the development of small-scale discrete auroral arc undulations on an isolated arc ~1–3 min prior to auroral breakup. In addition to examining the first onset of Pi1 power, we further examine and discuss the characteristics of Pi1 ULF power at each magnetometer station and their implications for locating substorm onset in the ionosphere in both time and space.

2. Methodology

[8] The Automatic Wavelet Estimation of Substorm Onset and Magnetic Events (AWESOME) [*Murphy et al.*, 2008, *Milling et al.*, 2008] technique uses a discrete wavelet transform (DWT) with a Meyer wavelet basis to characterize magnetometer time series. The AWESOME algorithm computes the onset of a ULF wave signal that is two standard deviations above the mean noise level calculated using a noise level for a preonset magnetically quiet time interval. This technique has the advantage of defining mathematically the ULF onset time instead of the more subjective determination of wave onset "by eye" which is often used.

[9] In this paper we identify and define auroral breakup as the time at which the preexisting east–west aligned discrete arc system is sufficiently distorted that the arc morphology is no longer confined to small perturbations around a constant latitude. For example, while arc undulations about a constant latitude would not indicate breakup, distortion and/or bending of the arc morphology which leads to destruction of the symmetry of east–west arcs in the auroral oval would define breakup. Where this is followed by westward expansion, this indicates the release of the WTS. By this definition, auroral breakup does not occur at the same time as expansion phase onset. We continue to use the classical Akasofu definition that "The first indication of a substorm is a sudden brightening of one of the quiet arcs lying in the midnight sector of the oval (or a sudden formation of an arc)" [*Akasofu*, 1977, pp. 7–8]. There are cases where equatorward arc brightening and/or breakup is not followed by the development of a global disturbance especially perturbation of the poleward boundary of the auroral oval.

[10] We define the time when the transverse ULF wave power rises above the mean quiet time ULF noise by two standard deviations (hereafter termed δb) as ULF wave onset at a particular magnetometer station. Note that the noise level is frequency dependent, since the power in a specific wavelet band is also frequency dependent. During complex or compound events which evolve as series of precursors or pseudobreakups, followed by a main onset and are often accompanied by subsequent intensifications, defining an appropriate quiet time can be subjective. However, even at such times it is still possible to determine the times of ULF wave intensifications around substorm onset. For isolated substorms, the use of a δb threshold above prestorm quiet time level has been shown to generate excellent results when compared to the onset location as determined by IMAGE FUV observations (see *Murphy et*

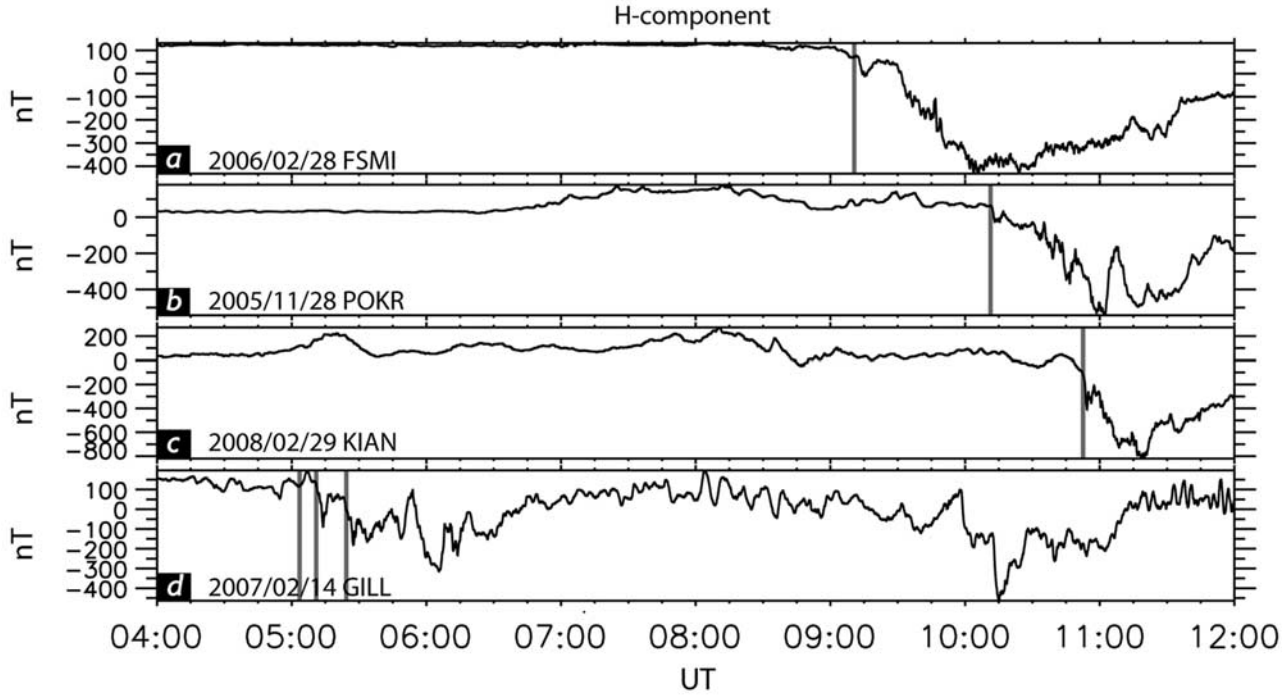

Figure 1. H component ground magnetometer magnetic fields from selected stations in the North American sector from (a) FSMI on 28 February 2006, (b) POKR on 28 November 2005, and (c) GILL on 14 February 2007, between 0400 and 1200 UT. The red vertical lines denote the onsets discussed in section 3.

al. [2008] for more details). Identifying auroral breakup in the THEMIS ASIs is somewhat easier so long as the skies are clear, though it is still difficult to define a threshold to uniquely identify when auroral features intensify. In this paper, we examine the first minute of optical onset using both the original ASI images and the difference between successive ASI images which are either 3 s or, in one case study, 6 s (the highest resolution between adjacent frames) apart. We present a number of case studies, and in each case, we present the contours of the time when Pi1/2 (24–96 s period) wave power exceeds the threshold for both substorm onsets or intensifications, together with false color images of the raw emission intensity and the difference in intensity between successive ASI images for the relevant ASI studies.

3. Case Studies

[11] We present case studies of the spatial and temporal evolution of optical and magnetic features for substorm periods. Figure 1 shows a summary of the H component magnetic data from one magnetometer station for each of these three days. The red lines denote the auroral and magnetic onsets presented in this paper. In the first two cases presented, we were able to successfully identify the substorm onset as characterized in ULF wave power in ground magnetometers which in each case was also associated with small-scale discrete auroral arc undulations. The last case presented illustrates features associated with a compound substorm event. This example shows evidence for activations at both high and low latitudes which may be evidence for multiple activation regions in some substorm events.

3.1. Case 1: 28 February 2006

[12] Figure 1a shows the overview of the intervals presented in this paper using data from the H component of the relevant stations (FSMI, POKR and GILL). Figure 2 shows the ground H (red), D (blue) and Z (black) component magnetometer data from selected THEMIS, CARISMA and GIMA stations in the Canadian and Alaskan sector between 0830 and 1000 UT on 28 February 2006 arranged from geomagnetic west to east and north to south. Clearly visible is the presence of an H component bay that has two stages to its development, indicative of substorm activity at ~0912 UT and a further development at ~0930 UT. Figure 3 shows the Pi2 (40–150 s period) FFT-filtered (Figure 3a) and the Pi1 (1–40 s period) FFT-filtered (Figure 3b) H component time series during the same time interval. It is difficult to determine whether there is a preferential first onset location for both the Pi2 and Pi1 signatures in these noisy time series. However, there does appear to be a time delay between Pi2 signatures observed at, for example, FTYK and DAWS prior to 0915 UT and those observed at ARCT and BETT around 0915 UT. Similarly, the onset of Pi1 signatures appears to be observed first at DAWS before the Pi1 activity at other stations, for example FTYK.

[13] Using the AWESOME algorithm, the first continuous set of wavelet coefficients that rise above the δb threshold of a presubstorm quiet time noise level are used to formally define the ULF wave onset time at each station for this event. The error in this timing is assumed to be half of the width of the time window in a given wavelet band. In this paper, we present inter-station onset timing results using

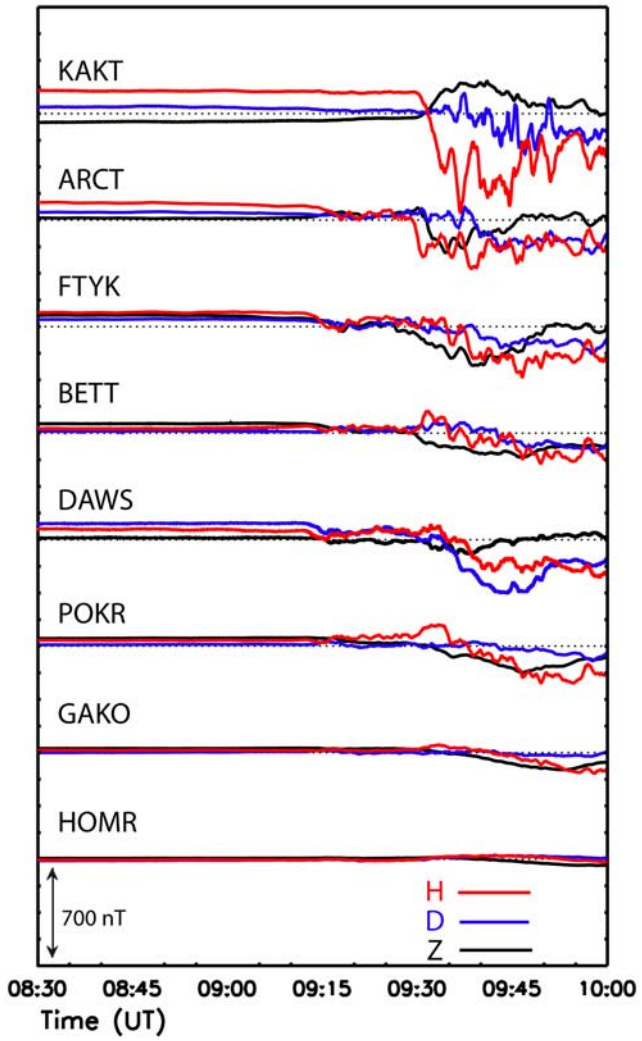

Figure 2. H, D, and Z component magnetic fields (red, blue, and black, respectively) from magnetometer stations in the Alaskan-western Canadian sector for 0830–1000 UT on 28 February 2006.

the first ULF wave band that exceeds threshold at any station. In this case, this occurs in the 24–96 s wavelet band (centered on 32 s) at FSIM, thus the errors are quoted as ±16 s.

[14] Figure 4 shows the result of wavelet power spectrum from FSIM, at which location both Pi1 and Pi2 (1–192 s) ULF waves are first observed, together with the wavelet coefficients from the 24–96 s wavelet bands from FSIM and GAKO. In each plot, the associated signal threshold is marked in blue corresponding to power at δb above preonset noise. Onset above this threshold is marked by the start of the red wavelet coefficients. Figure 4a clearly demonstrates the onset of long-period Pi1/short-period Pi2 ULF wave activity prior to the onset of activity in both higher and lower frequencies at FSIM. Furthermore, the wavelet coefficients from both FSIM and GAKO show that there is a time delay in the onset of the 24–96 s ULF wave power at longitudinally separated stations, the onset at GAKO being 196 s later than at FSMI. One point to note is that the onset of ULF wave power at FSMI at 0910:36 UT is ~2 min prior to the onset of the intensification of ULF wave power, which can be characterized by eye in Figure 3 around ~0912 UT. By using a formal procedure to determine onset, we eliminate subjective errors that the eye may introduce by focusing only on the largest change in ULF wave amplitude with time that will dominate a time series.

[15] Figure 5 (top) shows a 2D minimum curvature surface fit to the first onset time of 24–96 s period ULF waves during this substorm across 15 magnetometer stations, time defined relative to 0910:36 UT (±16 s), the first arrival time occurring at FSIM at that time. A clear and coherent onset pattern showing an "epicenter" with a localized first ionospheric arrival is clearly observed. An onset region for ULF waves in the ionosphere close to FSIM is revealed, bounded to the west and east by DAWS and YKC, respectively, and PTRS to the south. Figure 5 (bottom) shows (left) the false color original and (right) the 6 s differenced images from the WHIT ASI at three times, one minute apart. Small-scale auroral undulations appear to brighten on a weak arc to the north and east of the center of the WHIT field of view (FOV). Immediately evident from the ASI data is the emergence of optical beads in the WHIT FOV in the spatial region identified by the ULF magnetic wave onset, to the north of WHIT, and in a longitudinal region bounded by FSIM and DAWS (note there is no magnetometer data available for WHIT in this interval). The appearance of this auroral structure is closely related to the Pi1 onset location, being colocated both in time (~30 s following the onset of Pi1 pulsations at FSIM) and space (in the longitudinal region between DAWS-FSIM). During the subsequent 2–3 min, these features develop into auroral vortices (see auxiliary material Animation S1[1]), and a WTS subsequently forms (cf. Rae et al., submitted manuscript, 2008). Note also that the white patch in the final differenced image represent the effects of saturation in the image intensity.

[16] We compare the ground H, D and Z component magnetic bay structures with the ASI and long-period Pi1 waves with results from the SCW model detailed by *Cramoysan et al.* [1995]. Fitting the observed bays to this model, we can estimate the locations of the upward and downward FAC element meridians, and also estimate the central meridian of the SCW in relation a nonuniform grid represented by the available station coverage. The location of the central meridian lies between FTYK and EAGL and close to GAKO, and the upward FAC element between BETT and POKR. There is insufficient station coverage to infer an accurate location for the meridian of the downward FAC element, although it is most likely situated between GAKO and PTRS, i.e., assuming a symmetric SCW, to the east of DAWS. Finally, the electrojet latitude is inferred from the SCW analysis to be located between ARCT and FTYK. The estimated location of the downward FAC element is therefore found to be close to the location of both the Pi1 onset and the formation of small-scale optical auroral arc undulations, and shown in Figure 5 (top).

3.2. Case 2: 28 November 2005

[17] This interval was first presented by *Donovan et al.* [2007], and the event was identified by these authors to

[1]Auxiliary materials are available in the HTML. doi:10.1029/2008JA013559.

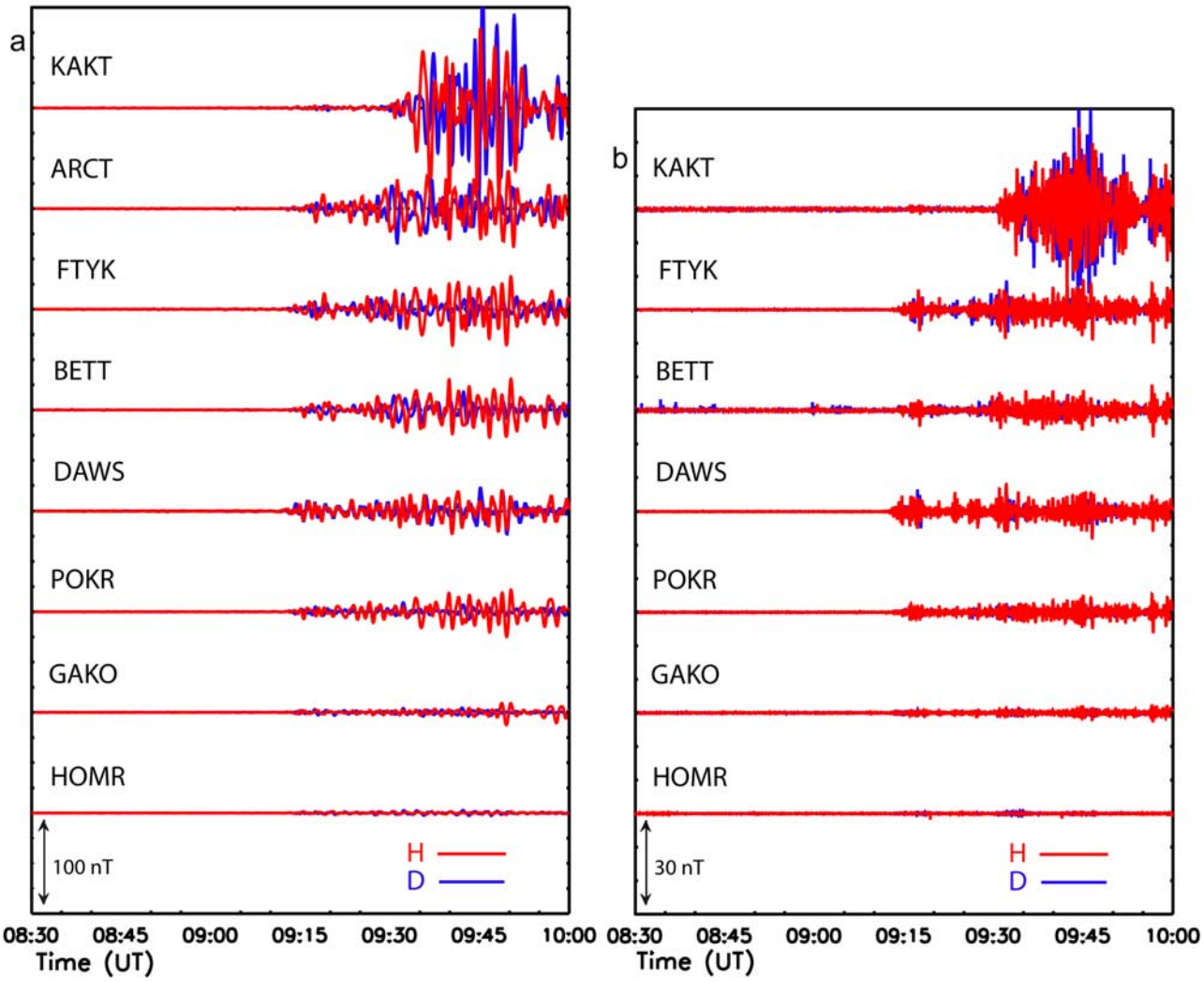

Figure 3. (a) Pi2 (40–150 s period) and (b) Pi1 (1–40 s period) filtered H, D, and Z component magnetic fields from selected stations in the Alaskan-western Canadian sector for 0830–1000 UT on 28 February 2006 in the same format as Figure 2.

most likely represent a pseudobreakup rather than a full substorm expansion phase onset. In this section we further analyze the optical ASI data and complete a detailed analysis of the accompanying magnetic signals using the AWESOME technique. Figure 1b shows an overview of this interval using the H component magnetic field observed at POKR, which recorded a magnetic bay of ~500 nT amplitude. Figure 6 (bottom) shows THEMIS ASI data from WHIT, together with the 24–96 s ULF onset contours (top) in the same format as Figure 5. Evident from Figure 6 is that the ULF long-period Pi1 (j = 6) epicenter is located in a longitudinal region that is encompassed by the stations BETT-POKR-EAGL-DAWS, epoch time zero and the onset of the Pi1 waves occurring at these stations at 1011:20 UT (±16 s). *Donovan et al.* [2007] identified the onset time as 1011:36 UT from 12 s differenced ASI images. In this paper, we reanalyze the ASI data and show differenced images that are 6 s apart. What is evident from Figure 6 is a small optical brightening close to the POKR site at 1011:30 UT. Auroral undulations with a scale size along the arc of 50–100 km appear, and develop in subsequent frames into larger azimuthal wavelength features before developing into auroral vortices as in the previous event (Figure 5). The epicenter of the Pi1/2 onset occurs contemporaneously with, and in the same location as, the development of auroral beads to within the error (±16 s).

3.3. Case 3: 14 February 2007

[18] There were several clear optical intensifications observed in the THEMIS GILL and FSMI ASI between 0457 and 0524 UT on 14 February 2007. In this paper we outline the capability of the AWESOME technique to distinguish between closely separated intensifications in Pi1 ULF power that are closely related to auroral arc structuring by concentrating on five intensifications around 0457 UT, 0500 UT, 0503 UT, 0510 UT and 0524 UT. Figure 7 shows the H component magnetometer data for selected stations in this interval. The intensification times marked by dashed lines, the last of which represents auroral breakup. Significant and repeated small-amplitude fluctuations were seen in the GILL magnetometer before the substorm onset and the development of a larger-scale

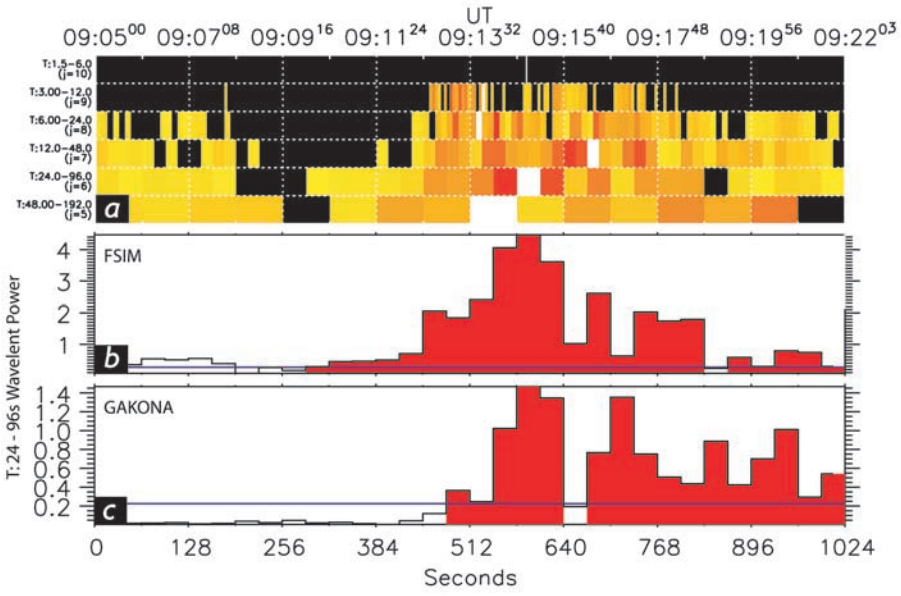

Figure 4. The AWESOME Discrete Wavelet Transform (DWT) analysis of the FSMI magnetometer data. (a) The wavelet power spectra as a function of frequency (j) and time. The lower *x* axis denotes time in seconds starting from 0905 UT, the upper *x* axis denotes UT time, and the *y* axis denotes frequency. Color denotes wavelet coefficient power, where yellow is low power and red is the highest power normalized independently to the highest power in each frequency band (white). (b and c) The amplitude of the wavelet coefficients from FSIM and GAKO in the j = 6 (24–96 s) period wavelet band. The blue horizontal line denotes the determined noise threshold, and the red bars indicate the continuous enhancement of wavelet coefficient past that noise level.

magnetic bay and SCW structure across the array following the susbstorm onset at around 0524 UT.

[19] Figure 8 shows the 24–96 s wavelet band ULF wave power from three representative stations GILL, ISLL and TPAS normalized to the preonset δb ULF wave power (blue horizontal line) in the same format as Figure 4. The AWESOME technique is able to distinguish four discrete ULF wave onsets above the prestorm noise threshold at both TPAS and ISLL, and 3 discrete ULF wave onsets at GILL in advance of the auroral breakup at ~0524 UT. There is some evidence that the GILL magnetometer observes enhanced power during the first intensification identified in ISLL and TPAS at ~0458 UT (purple vertical lines). However, a full waveform (corresponding to two wavelet coefficient blocks) is not observed to rise above the prestorm onset noise level, and therefore we do not establish a formal AWESOME timing for this first activation. The second activation (red vertical lines) around ~0500 UT is clearly observed in all three magnetometers within one wavelet band of each other. The third activation around ~0503 UT is observed to occur first at TPAS, and then subsequently at ISLL and GILL. The fourth and largest preonset activation occurs around 0510 UT first at TPAS, and then at ISLL and GILL.

[20] Figure 9 shows the minimum curvature fit to the long-period Pi1 onset times determined from the magnetometers for these four preonset ULF wave activations (left) together with a representative ASI image from FSMI and GILL close to the activation (right). Interestingly, all four preonset ULF activations have markedly different characteristics. The first activation at 0457:36 UT (±16 s) appears to have two distinct and separate locations of activity: one around PBQ and the other close to TPAS. There are two small optical features observed around 0458 UT; the development of a north–south arc structure to the north and east of GILL, and an optical intensification close to the TPAS-RABB magnetometers which may be the optical counterpart of the ULF activity.

[21] The second activation occurs first at FCHU at 05:00:16 (±16 s), and propagates to lower latitudes; there is not sufficient station resolution with which to investigate any poleward progression. This activation appears to be coincident with the brightening and further development of the north–south arc close to FCHU.

[22] The third ULF activation is more clearly observed, and has a well-defined epicenter close to TPAS. This location is consistent with the region characterized by the formation of small-scale auroral undulations along a preexisting discrete arc, the temporal development of which is shown in Figure 10a in the same format as the optical observations shown in Figures 5 and 6. The optical undulations shown in Figure 10a, in contrast to Cases 1 and 2 do not develop into larger-scale vortices and are not followed ~minutes later by auroral breakup.

[23] The fourth ULF activation at 0509:20 UT (±16 s) occurs close to the PINA magnetometer, and is closely followed by ULF wave power exceeding the threshold at TPAS as the ULF wave onset time progresses north. One interesting point to note is that the time that the onset of 24–96 s ULF wave power exceeds the threshold is observed contemporaneously at FCHU, PBQ and ISLL, in significantly disparate locations. Interestingly, GILL is the last

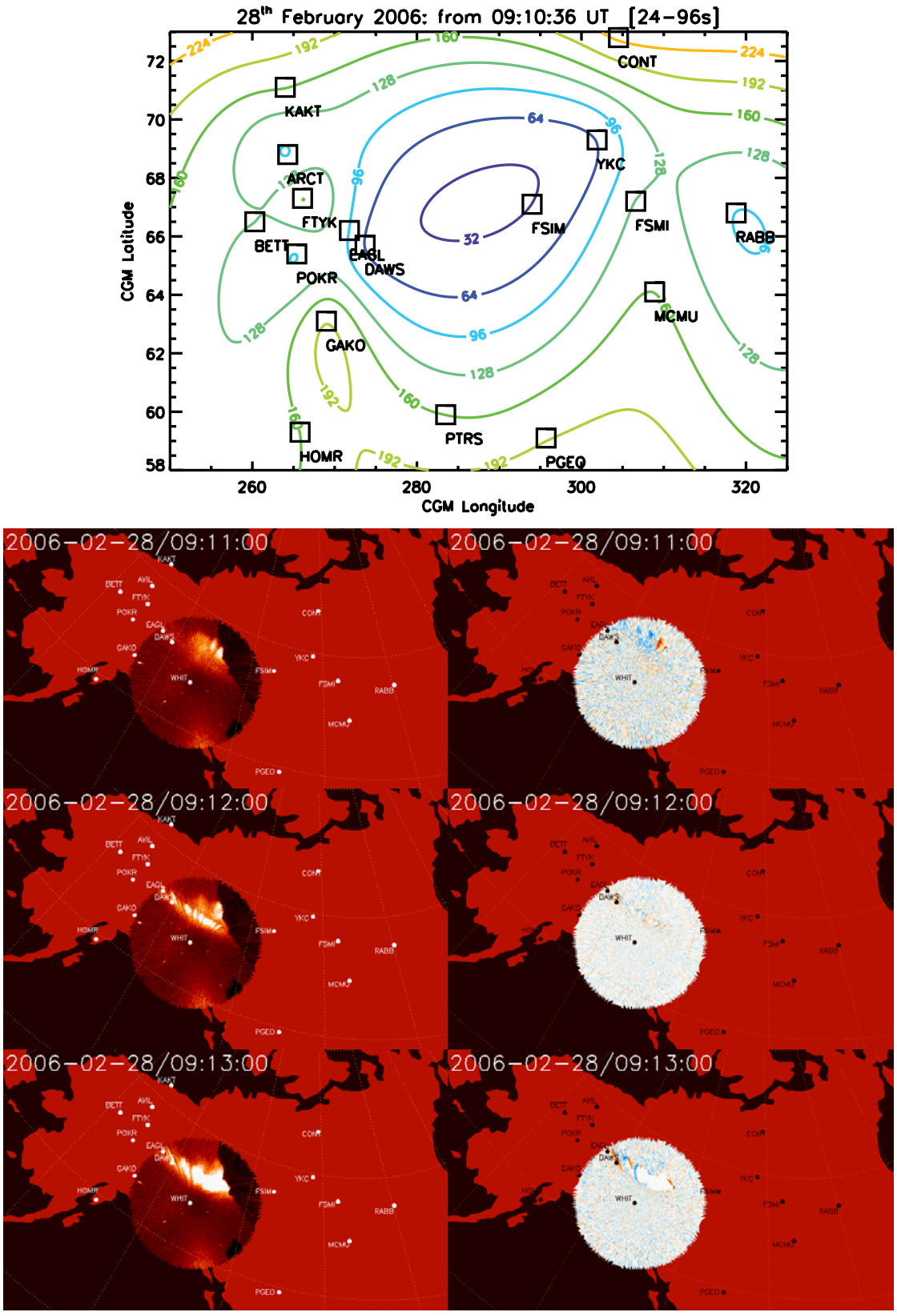

Figure 5. (top) Minimum curvature surface fit to the J = 6 24–96 s ULF wave onset times using the AWESOME technique on the 15 magnetometer stations used on 28 February 2006; contours are 32 s apart. The approximate locations of the upward and downward field-aligned current elements and the electrojet latitude are denoted by the gray symbols and arrow. (bottom) Selected false color (left) original and (right) difference images from the THEMIS WHIT ASI from 0911:00 UT, 0912:00 UT, and 0913:00 UT. The locations of the magnetometers used in this study are marked.

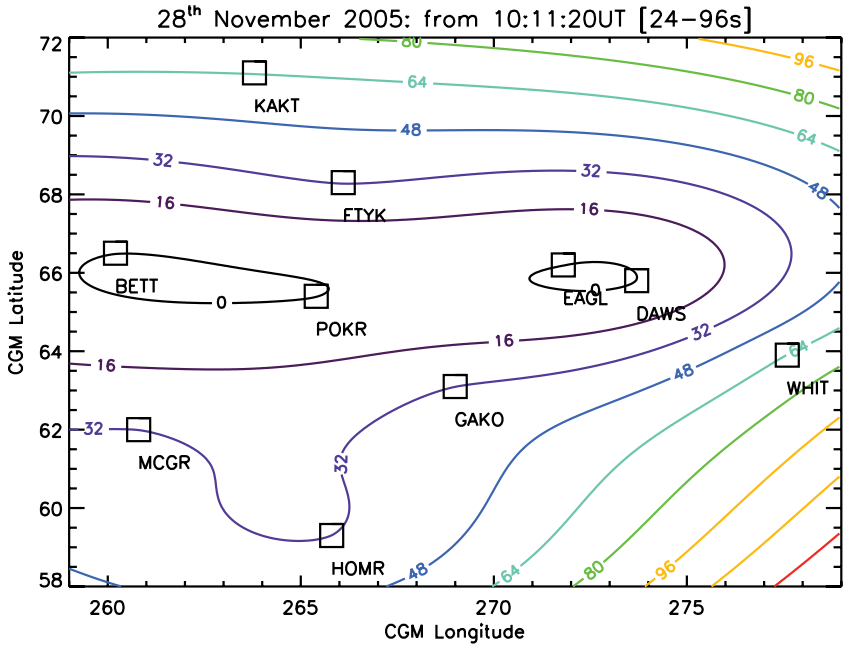

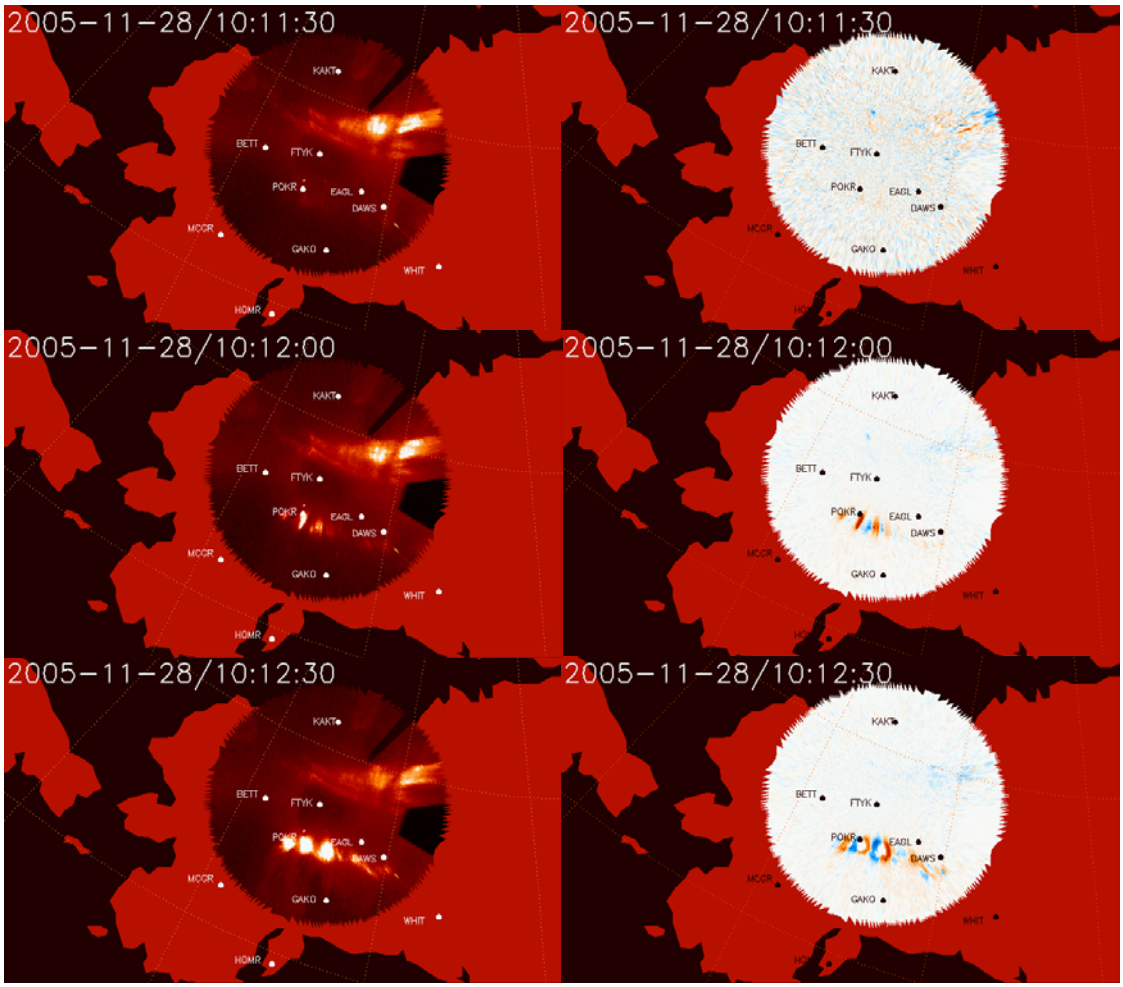

Figure 6. (top) Minimum curvature surface fit to the J = 6 24–96 s ULF wave onset times using the AWESOME technique on the 10 magnetometer stations used on 28 November 2005 in the same format as Figure 5; contours are 16 s apart. (bottom) Selected false color (left) original and (right) difference images from the THEMIS FTYK ASI from 1011:30 UT, 1012:00 UT, and 1012:30 UT. The locations of the magnetometers used in this study are marked.

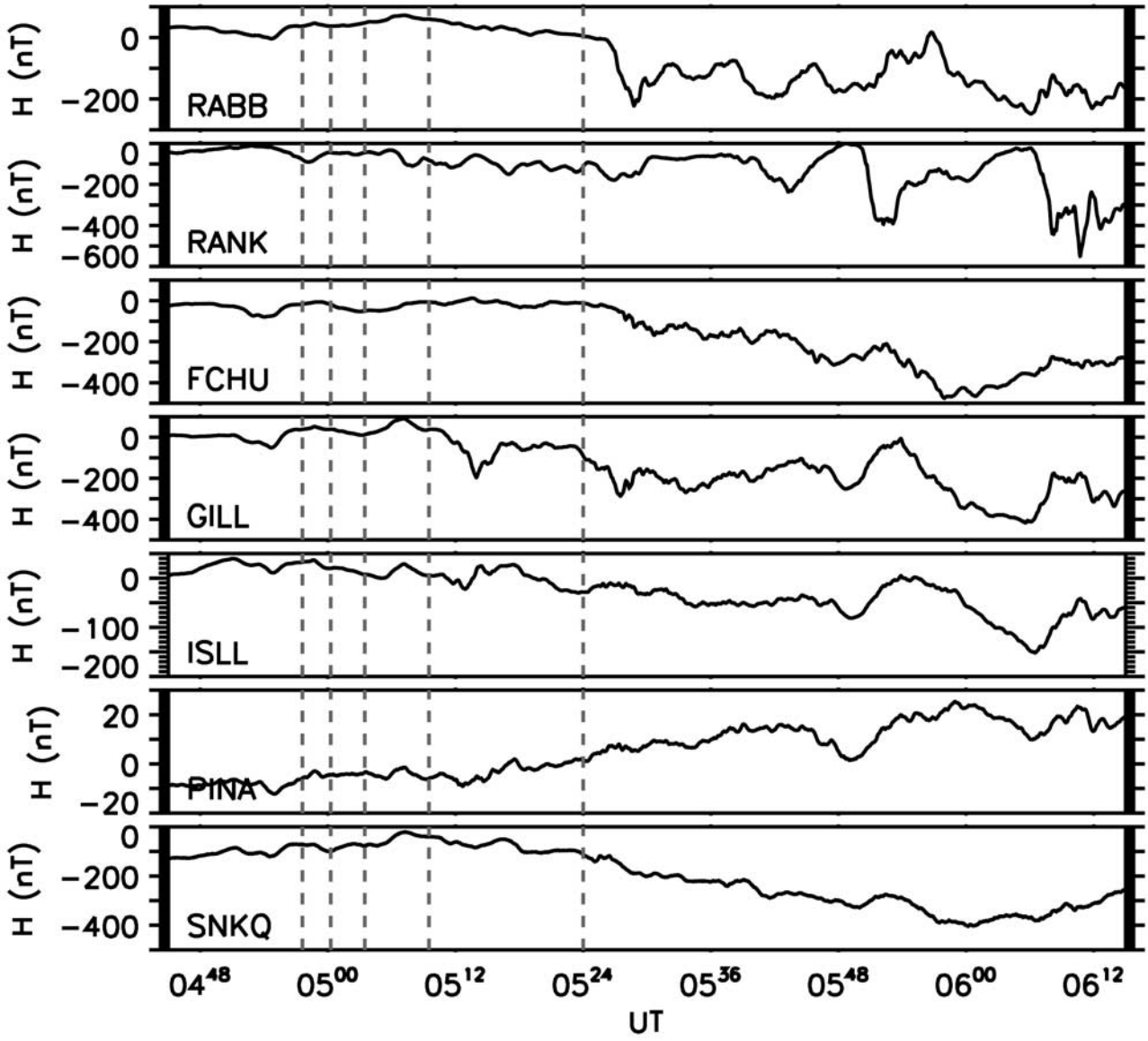

Figure 7. H component ground magnetometer data from 0445 to 0615 UT on 14 February 2007. The stations shown run from west to east and north to south. The red dashed lines denote the Pi1 ULF wave onsets discussed in section 3.3.

station to see ULF wave activation. Optical undulations are observed between the TPAS-ISLL magnetometers, and this time, these undulations do develop into larger-scale vortices (Figure 10b). Indeed, a localized surge is formed in the ASI images, but this does not expand and instead dies down. An interesting point to note in the differenced images in Figure 10b is that there is a signature of auroral intensity fluctuations on a higher-latitude arc close to FCHU, which may be responsible for the dual ULF wave epicenter in this event. In Animation S2, these are associated with equatorward moving auroral patches which propagate along a north–south aligned arc. Finally, Figure 10c shows the time sequence of 3 frames of ASI data one minute apart during the substorm onset at ~0524 UT. This activation results in the full auroral breakup and hence we associate it with expansion phase onset. Interestingly, immediately overhead in the FSMI and GILL ASIs, undulations along a bright onset equatorward arc are generated during an intensification in ULF wave power at the GILL magnetometer. However, at this stage in the evolution of this compound event, the ULF wave power already exceeds the predefined δb threshold. It is not obvious how to define a new threshold with which to time the ULF wave power intensification with AWESOME. It is clear from the 24–96 s ULF wave power observed at GILL that there is significant ULF wave intensification at 0524 UT (see Animation S2).

4. Discussion

[24] We present results from a new method with which to time and locate the first signatures of expansion phase onset utilizing the newly developed AWESOME algorithm as applied to ground magnetometer data detailed by *Murphy et al.* [2008] and used by *Milling et al.* [2008] and Rae et al.

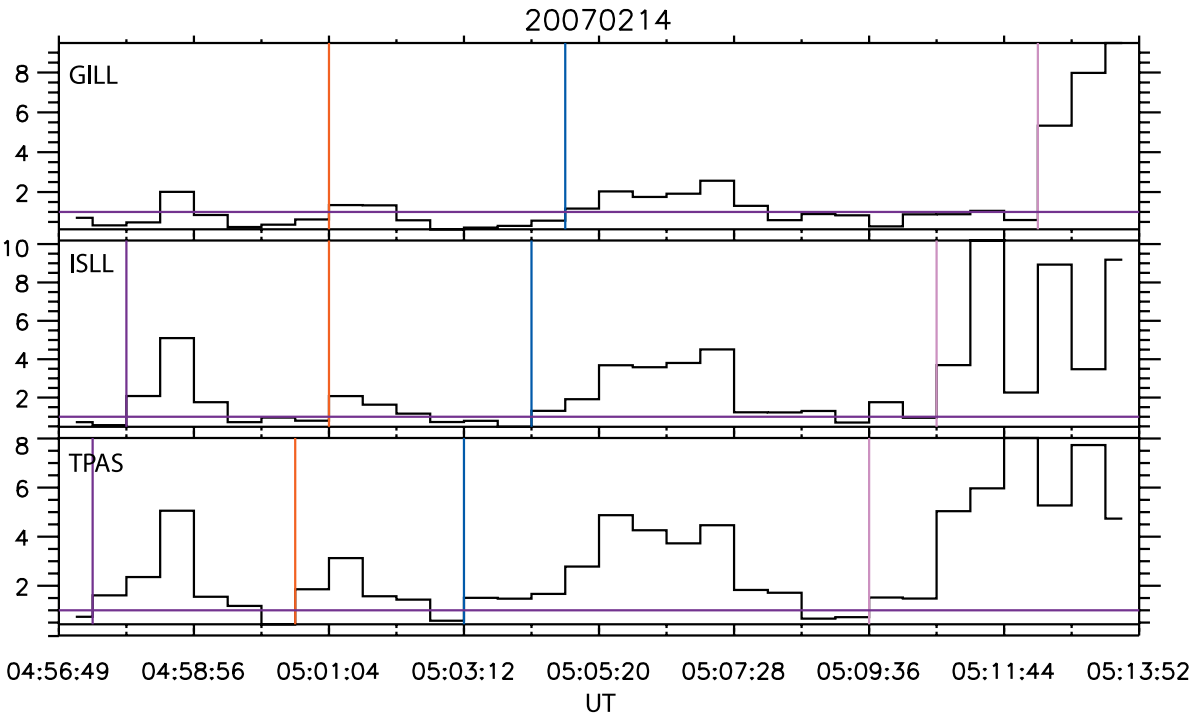

Figure 8. The 24–96 s Pi1/2 wavelet determined ULF wave power normalized to the prestorm quiet time plus two standard deviation noise level for GILL, ISLL, and TPAS magnetometers. The colored lines denote the onset of Pi1/2 ULF waves above the normalized threshold (horizontal blue lines).

(submitted manuscript, 2008) several minutes prior to auroral breakup. In this paper, we compare the location of optical onset in THEMIS white light ASI data with the long-period Pi1/short-period Pi2 (24–96 s period wavelet band) ULF wave onset as determined by the AWESOME technique. Using these techniques, we find that the onset of Pi1/2 ULF wave activity is coincident in both time and space with the formation and evolution of small-scale undulations along the discrete most equatorward arcs prior to auroral breakup.

[25] *Milling et al.* [2008] presented discrete wavelet analysis of the onset of Pi1 ULF waves across the CARISMA, THEMIS GMAG and CANMOS arrays during a small isolated substorm and found that the onset of these ULF waves initiated at, and propagated coherently away from, an epicenter in the ionosphere. *Milling et al.* [2008] showed that the long-period Pi1 wavelet band can be used to determine both the time and location of ULF wave onset in the ionosphere to an accuracy of ~tens of seconds, providing clear evidence that the long-period Pi1 must be considered as an important element of the ULF waves excited during expansion phase onset. Furthermore, by comparing the ground magnetic bay structure to a simple SCW model [e.g., *Cramoysan et al.*, 1995], *Milling et al.* [2008] also showed that the epicenter of the long-period Pi1 ULF waves occurred in a region where the downward FAC element of the SCW subsequently formed. Case 1 presented in this paper also demonstrates the same relationship.

[26] *Murphy et al.* [2008] presented clear observations of the relative timing between the onset of Pi1/2 ULF waves with optical onset from the Frey substorm database [*Frey et al.*, 2004; *Frey and Mende*, 2007] as determined from the IMAGE-FUV instrument. In each of the case studies presented by Murphy et al., these authors determined that the onset of 12–48 s or 24–96 s ULF waves as determined by the AWESOME algorithm occurred 4–12 min earlier than the colocated optical onset determined from global satellite-based in situ auroral imaging observations. The results of Murphy et al. provide further clear evidence that the onset of ULF waves in the long-period Pi1/short-period Pi2 band occur first at, and propagate clearly away from, a single epicenter in the ionosphere during isolated substorm expansion phase onsets. In compound events, there appears to be two or more discrete epicenters that correspond to the number of optical intensifications present (see Figure 9 (bottom)).

[27] In this paper, we present several case studies which extend the auroral onset correlation reported by *Murphy et al.* [2008] to examine the relationship of onset arc fine auroral structure to the Pi1 ULF wave onset using data from the THEMIS ASI and GMAG networks and CARISMA. Specifically, we compare Pi1 ULF wave onset location to small-scale (~50–70 km) optical undulations forming along the most equatorward preexisting auroral arcs. Our results indicated that these optical and Pi1 magnetic features are closely related.

[28] Small-scale auroral features like the beads that are reported here have been previously discussed by *Donovan et al.* [2007], *Liang et al.* [2008] and Rae et al. (submitted manuscript, 2008) as being intimately linked to substorm expansion phase onset. *Liang et al.* [2008] and Rae et al. (submitted manuscript, 2008) presented strong evidence that the formation and evolution of small-scale auroral undulations corresponded to the first signatures of expansion phase

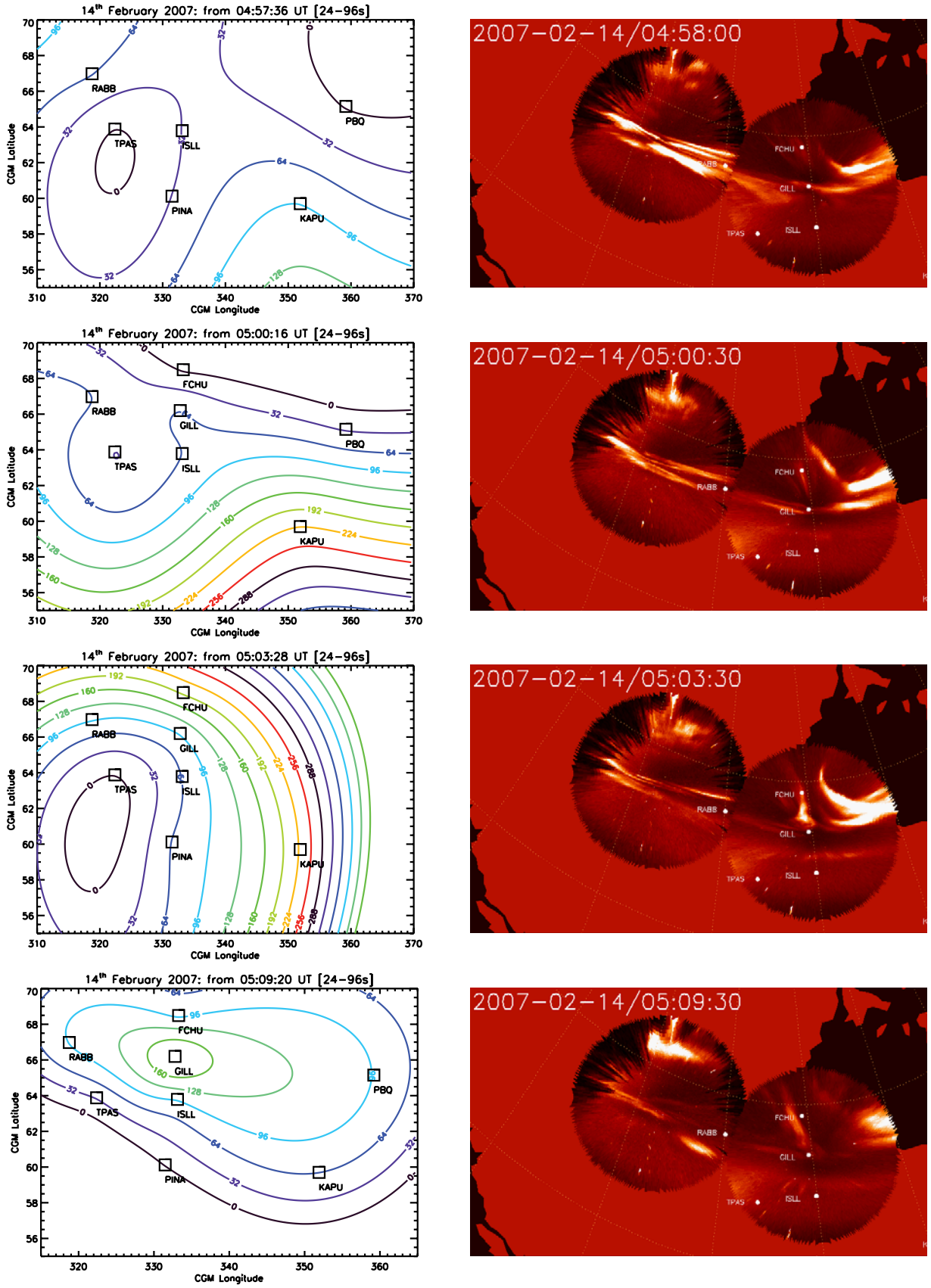

Figure 9. Optical and Pi1 magnetic data on 14 February 2007. (left) Contour plots of the Pi1 onset observed by the magnetometers shown. (right) False color images from the FSMI and GILL ASIs from times just after the onset of the contours in the left plots.

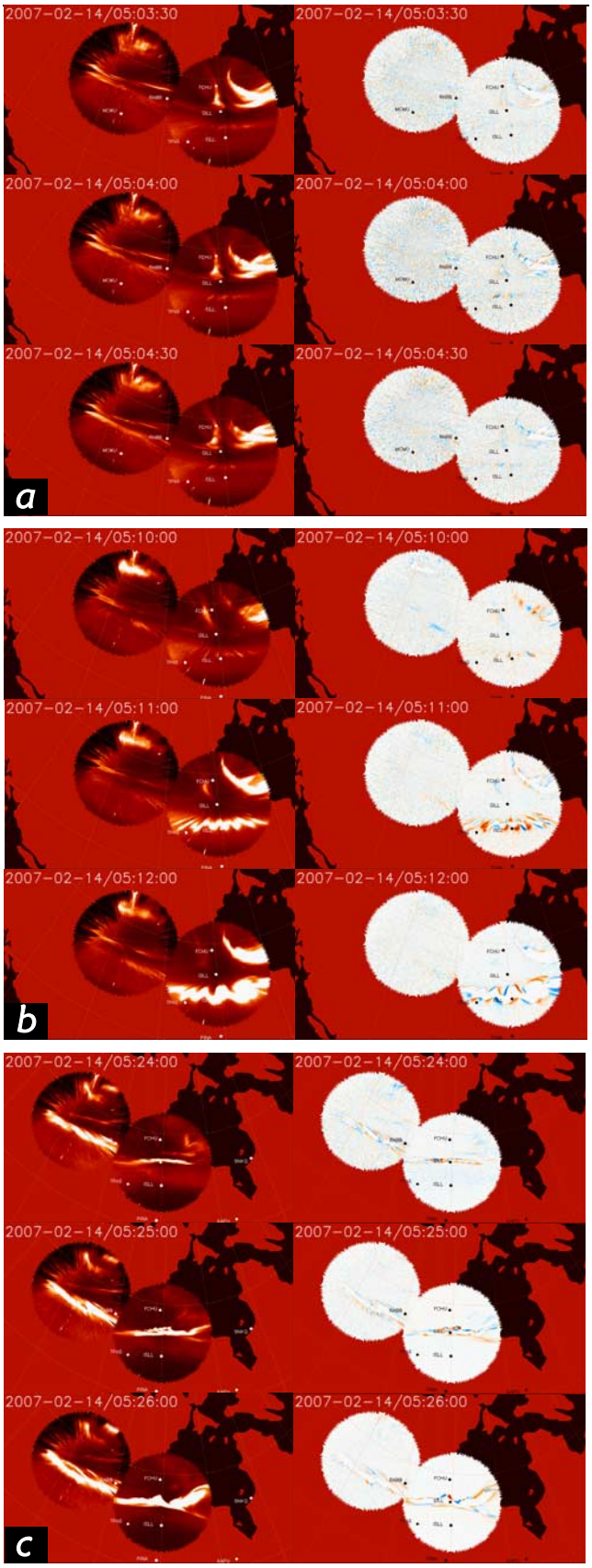

Figure 10. On the left are false color images and on the right are 3 s difference images from the FSMI and GILL ASIs for the three onsets from (a) ~0503 UT, (b) ~0510 UT, and (c) ~0524 UT. Successive frames are 30 s apart for Figure 10a and 1 min apart for Figures 10b and 10c.

onset in the ionosphere. *Liang et al.* [2008] characterized the azimuthal wave numbers of the optical beads along the arc as being m = 100–300, and that the time scale of their intensification was 10–30 s. Rae et al. (submitted manuscript, 2008) established that the evolution of the arc undulations underwent an inverse spatial cascade from ~50–70 km arc ripples to >100 km vortices as previously reported by *Friedrich et al.* [2001], though presented at much higher temporal resolution than available in their study. The vortices appear to subsequently develop a nonlinear and wrapped character [e.g., *Voronkov et al.*, 2000; *Lyons et al.*, 2002] before they eventually propagate poleward to the location of the more poleward preexisting arc system.

[29] In the first two cases presented here, we have established that Pi1 ULF waves can be used to map the first magnetic disturbances associated with expansion phase onset. In these cases 1 and 2, the Pi1 ULF power was colocated with the auroral undulations which preceded the development of substorm onset and auroral breakup by ~3 min and ~1 min, respectively. We believe that both the Pi1 waves and the auroral undulations, based on their location relative to more poleward preexisting discrete arcs and the closed contours of Pi1 power, represent the auroral signatures of near-Earth plasma sheet activations. This assertion is consistent with the findings of Rae et al. (submitted manuscript, 2008), where such auroral beads were found to map close to the inner edge of the plasma sheet via comparison to the cut-off in 4861Å emissions. In both cases 1 and 2, these auroral undulations breakup and develop into vortices and evolve over the following ~3 min before the WTS is released; the WTS in case 2 being localized since this event is most probably a pseudobreakup [cf. *Donovan et al.*, 2007].

[30] Importantly, the closed Pi1 contours and localization of the auroral arc undulations/beads at relatively low latitudes indicate a first ionospheric activation during substorm expansion at the equatorward edge of the oval. While the activation of the equatorward arc has been long-established as the ionospheric indication of onset [cf. *Akasofu*, 1964, 1977], our observations in cases 1 and 2 provide evidence of the nature of these prebreakup optical and magnetic signatures. Significantly, these equatorward Pi1 waves and arc undulations develop for 1–3 min prior to breakup. During this period, the more poleward preexisting discrete arc system remains undisturbed. This suggests that the processes responsible for substorm onset either map to this most equatorial arc latitude, or if they propagate to that location from a more distant source, do not perturb the preexisting more poleward arcs., which presumably map to the CPS.

[31] Worthy of note is that Case 3 demonstrates an example which illustrates the fact that many substorm onsets are compound in nature. Indeed, Figure 7 shows the development of some localized magnetic activations close to GILL and the Churchill meridian, which do not lead directly to

substorm onset auroral breakup. This activity continues for ~30 min before an activation occurs which leads to auroral breakup. Figures 9 and 10 show that prior to onset, auroral disturbances and arc brightenings are clearly associated with ULF wave onsets captured in the Pi1 band. More interestingly, the activations at ~0503 UT (Figure 10a) and around 0510 UT (Figure 10b) clearly show the development of auroral undulations and beads along the most equatorward discrete arc in the same manner as Cases 1 and 2. However, for these two activations substorm breakup does not immediately follow. At 0503 UT, arc undulations develop, but evolution into auroral vortices does not occur and eventually the arc fades. At 0510 UT, similar arc undulations again appear on the most equatorward arc. In this case, an inverse spatial cascade to larger-scale beads and eventually development into vortices is observed. Moreover, a localized auroral surge is seen local to the vortices, but this surge decays and does not expand poleward nor westward as a WTS. Only finally at ~0524 UT does an activation which leads to auroral breakup occur. In this case, arc undulations again appear overhead in the FSMI and GILL ASI FOV, but clear vortices do not develop. Between 0525 and 0526 UT, signatures of the WTS enter the GILL FOV from the east, suggesting that the arc evolution resulting in auroral breakup and substorm onset occurred further to the east outside the FOV of these cameras. *Aikio et al.* [1999] presented comprehensive studies of the ionospheric, geosynchronous and midtail features of a series of pseudobreakups and substorm expansion phase onsets, and concluded that there was no qualitative distinction between pseudobreakups and substorm onsets, rather there is a continuum of states between these two classifications. This is consistent with the results presented in Case 3.

[32] In fact, closer inspection of Figures 9 and 10 (see also Animation S2) also shows clear evidence for north–south auroral structures or streamers between FCHU and GILL along the Churchill Line [cf. *Henderson et al.*, 1998]. Such north–south structures have been associated with earthward flows generally assumed to be in the form of bursty bulk flows (BBFs) [*Angelopoulos et al.*, 1992], arising from reconnection at a NENL [*Lam et al.*, 2006; *Zesta et al.*, 2000, 2006]. The north–south streamers seen in Figure 10a near the central meridian of the GILL ASI FOV show clear equatorward propagation of localized intensifications, this being revealed particularly clearly in the top right region of the FOV of the GILL camera in 3 s differenced images at 0510:00 UT. This provides strong evidence that earthward flow bursts are being generated during this interval. Indeed, in Figure 10b it appears that in the minutes subsequent to 0510 UT that both north–south auroral streamers, perhaps arising from NENL reconnection, and undulations on the most equatorward arc, perhaps related to near-Earth plasma sheet instabilities, coexist. One suggestion is that during this event, two activation centers located both in near-Earth space and at the NENL may be operating simultaneously. An alternate scenario is that several reconnection points in a significantly stretched tail geometry may be occurring independently at different times, successively occurring and being stifled [e.g., *Mishin et al.*, 2001] until the substorm is successfully initiated. In this case, the stability of the more poleward arc system mapping to the plasma sheet must be successfully explained (e.g., Rae et al., submitted manuscript, 2008).

[33] Perhaps more surprising, is that despite these different centers of activation, a substorm onset characterized by auroral breakup and generation of the WTS only occurs following several activations. In fact, the undulations which develop repeatedly on the most equatorward discrete arc appear, evolve and disappear cyclically to different extents at different times (for example, the undulations at 0503 UT and 0510 UT). This suggests that the near-Earth plasma sheet processes may generate a signature of auroral undulations on the most equatorward arc, but this is clearly not a sufficient condition for the development of expansion phase onset. Finally, for case 3, the disturbances do ultimately develop an auroral breakup, but this appears to develop to the east of the FOV of the GILL ASI, and so it is not possible for us to establish in this case based on auroral and magnetic measurements in the ionosphere, whether the substorm was triggered uniquely via either the CD or NENL paradigm. The most equatorward discrete arc ahead of the WTS does however, appear to show evidence of structuring similar to the auroral undulations which characterize onset in cases 1 and 2.

5. Conclusions

[34] We present results from the AWESOME technique as applied to ground magnetometer data with comparisons of small-scale auroral features along onset arcs following substorm expansion phase onset. We present three case studies of the temporal evolution of these small-scale auroral undulations together with counterpart long-period Pi1/short-period Pi2 ULF pulsations using the AWESOME technique [*Murphy et al.*, 2008]. Remarkably, in two of these case studies the onset of Pi1 ULF waves is observed both contemporaneously and in the same location as the small-scale auroral features that subsequently develop into vortices prior to the release of the WTS. In the third case study, we find that multiple activation sites can be studied and differentiated using careful analysis of ground-based magnetometer data.

[35] In this paper we define auroral breakup as asymmetric distortion of the preexisting east–west aligned discrete arc system away from its central latitude. We continue to use the classical Akasofu optical description to define substorm onset. The relationship of the Pi1 initiation and the auroral arc undulations/beads to the physics of the processes triggering expansion phase onset remains to be determined. On the basis of the evidence presented here, it is likely that these disturbances, which precede both onset and auroral breakup, are intimated related to substorm expansion phase initiation. The relative timing between the Pi1 initiation and subsequent auroral breakup must be successfully explained by any substorm model.

[36] It is clear that the Pi1 wave onsets we report here can be related to the initiation of the development of preonset auroral undulations/beads in both space and time on the most equatorward arc prior to substorm expansion phase onset. However, they can also be related to auroral brightenings and other activations, which may also be onset-related. Likely, the Pi1s are related to Alfvén waves in both

cases, however further studies of the magnetospheric counterparts for both the preonset auroral beads, as well as Pi1s in general, are warranted. In terms of the substorm process, and on the basis of the evidence shown in this paper, we propose that it is possible for many substorms to be characterized by activity and activations at both the near-Earth plasma sheet and NENL locations, perhaps simultaneously. Given the potential that these centers may activate within minutes of each other, or less, as illustrated in case 3, we suggest that such dual activation behavior may have contributed to continuing the lively debate seeking a single trigger location for all substorms. Of course, to resolve this issue requires the addition of in situ monitoring such as those offered by the THEMIS probes. However, the Pi1 ULF wave results presented in this paper demonstrate the value and utility of using ULF wave power especially when combined with optical auroral observations, for diagnosing the 2-D structure of substorm activations in the ionosphere. Moreover, since Pi1 ULF waves do not depend on the existence of clear skies, at times the onset identification technique offered by AWESOME offers crucial information enabling the two competing substorm paradigms to be differentiated.

[37] The decade-long search to answer the initiation of substorm expansion phase is a cause of considerable controversy, and the primary objective of the THEMIS mission, and central to this mission is the ability to time and locate physical phenomena on the ground and in space to an accuracy of ~30 s [*Sibeck and Angelopoulos*, 2008]. The application of the AWESOME technique to conjugate ULF wave onset in, for example, THEMIS FGM probe data may offer the most realistic method to resolve the "2-minute problem" of expansion phase onset available to date.

[38] **Acknowledgments.** CARISMA is operated by the University of Alberta and funded by the Canadian Space Agency. THEMIS is funded by NASA contract NAS5-02099. GIMA data are provided by the Geophysical Institute of the University of Alaska Fairbanks, and the Canadian Magnetic Observatory System (CANMOS) network, maintained and operated by the Geological Survey of Canada, also provided data used in this study.

[39] Wolfgang Baumjohann thanks Victor Sergeev and another reviewer for their assistance in evaluating this paper.

References

Akasofu, S. I. (1964), The development of the auroral substorm, *Planet. Space Sci.*, *12*(4), 273–282, doi:10.1016/0032-0633(64)90151-5.

Akasofu, S. I. (1977), *Physics of Magnetospheric Substorms*, D. Reidel, Dordrecht, Netherlands.

Angelopoulos, V. (2008), The THEMIS mission, *Space Sci. Rev.*, doi:10.1007/s11214-008-9336-1, in press.

Angelopoulos, V., W. Baumjohann, C. F. Kennel, F. V. Coroniti, M. G. Kivelson, R. Pellat, R. J. Walker, H. Lühr, and G. Paschmann (1992), Bursty bulk flows in the inner central plasma sheet, *J. Geophys. Res.*, *97*(A4), 4027–4039.

Angelopoulos, V., et al. (2008a), Tail reconnection triggering substorm onset, *Science*, *321*, 931–935, doi:10.1126/science.1160495.

Angelopoulos, V., et al. (2008b), First results from the THEMIS mission, *Space Sci. Rev.*, doi:10.1007/s11214-008-9378-4, in press.

Arnoldy, R. L., et al. (1987), Simultaneous measurement of aurora-related, irregular magnetic pulsations at northern and southern high latitudes, *J. Geophys. Res.*, *92*(A11), 12,221–12,232, doi:10.1029/JA092iA11p12221.

Atkinson, G. (1967), Current system of geomagnetic bays, *J. Geophys. Res.*, *72*(23), 6063–6067, doi:10.1029/JZ072i023p06063.

Bösinger, T. (1989), On the spectral index of the Pi1B power spectrum, *Ann. Geophys.*, *7*(4), 375–386.

Bösinger, T., and A. G. Yahnin (1987), PI1B type magnetic pulsation as a high time resolution monitor of substorm development, *Ann. Geophys., Ser. A*, *5*(4), 231–237.

Cramoysan, M., et al. (1995), The use of a model current wedge in the determination of the position of substorm current systems, *Ann. Geophys.*, *13*(6), 583–594, doi:10.1007/s00585-995-0583-0.

Donovan, E., et al. (2007), The azimuthal evolution of the substorm expansive phase onset aurora, in *Substorms VIII: Proceedings of the 8th International Conference on Substorms*, pp. 55–60, Univ. of Calgary Press, Calgary, Canada.

Frey, H. U., and S. B. Mende (2007), Substorm onsets as observed by IMAGE-FUV, in *Substorms VIII: Proceedings of the 8th International Conference on Substorms*, pp. 71–75, Univ. of Calgary Press, Calgary, Canada.

Frey, H. U., S. B. Mende, V. Angelopoulos, and E. F. Donovan (2004), Substorm onset observations by IMAGE-FUV, *J. Geophys. Res.*, *109*, A10304, doi:10.1029/2004JA010607.

Friedrich, E., et al. (2001), Dynamics of the substorm expansive phase, *J. Geophys. Res.*, *106*(A7), 13,145–13,163, doi:10.1029/2000JA000292.

Henderson, M. G., G. D. Reeves, and J. S. Murphree (1998), Are north–south aligned auroral structures an ionospheric manifestation of bursty bulk flows?, *Geophys. Res. Lett.*, *25*(19), 3737–3740, doi:10.1029/98GL02692.

Hones, E. W., et al. (1970a), Poleward expansion of auroral oval and associated phenomena in magnetotail during auroral substorms. 1, *J. Geophys. Res.*, *75*(34), 7060–7074, doi:10.1029/JA075i034p07060.

Hones, E. W., et al. (1970b), Poleward expansion of auroral oval and associated phenomena in magnetotail during auroral substorms, *Eos Trans. AGU*, *51*(4), 402.

Jacobs, J. A., et al. (1964), Classification of geomagnetic micropulsations, *J. Geophys. Res.*, *69*(1), 180–181, doi:10.1029/JZ069i001p00180.

Lam, M. M., M. Pinnock, and E. F. Donovan (2006), Observations of nightside magnetic reconnection during substorm growth and expansion phases, *J. Geophys. Res.*, *111*, A05209, doi:10.1029/2005JA011356.

Lessard, M. R., et al. (2006), Nature of Pi1B pulsations as inferred from ground and satellite observations, *Geophys. Res. Lett.*, *33*, L14108, doi:10.1029/2006GL026411.

Lester, M., et al. (1983), Polarization patterns of Pi 2 magnetic pulsations and the substorm current wedge, *J. Geophys. Res.*, *88*(A10), 7958–7966, doi:10.1029/JA088iA10p07958.

Liang, J., et al. (2008), Intensification of preexisting auroral arc at substorm expansion phase onset: Wave-like disruption during the first tens of seconds, *Geophys. Res. Lett.*, *35*, L17S19, doi:10.1029/2008GL033666.

Lui, A. T. Y. (1991), A synthesis of magnetospheric substorm models, *J. Geophys. Res.*, *96*(A2), 1849–1856, doi:10.1029/90JA02430.

Lyons, L. R., et al. (2002), Relation of substorm breakup arc to other growth-phase auroral arcs, *J. Geophys. Res.*, *107*(A11), 1390, doi:10.1029/2002JA009317.

Mann, I. R., et al. (2008), The CARISMA array in the THEMIS era, *Space Sci. Rev.*, in press.

McPherron, R. L., et al. (1973), Satellite studies of magnetospheric substorms on August 15, 1968. 9. Phenomenological model for substorms, *Eos Trans. AGU*, *54*(4), 206.

Mende, S., et al. (2008), The THEMIS array of ground based observatories for the study of auroral substorms, *Space Sci. Rev.*, in press.

Milling, D. K., et al. (2008), Ionospheric localization and expansion of long-period Pi1 pulsations at substorm onset, *Geophys. Res. Lett.*, *35*, L17S20, doi:10.1029/2008GL033672.

Mishin, V. M., T. Saifudinova, A. Bazarzhapov, C. T. Russell, W. Baumjohann, R. Nakamura, and M. Kubyshkina (2001), Two distinct substorm onsets, *J. Geophys. Res.*, *106*(A7), 13,105–13,118, doi:10.1029/2000JA900152.

Murphy, K. R., I. J. Rae, I. R. Mann, D. K. Milling, C. E. J. Watt, L. Ozeke, H. U. Frey, V. Angelopoulos, and C. T. Russell (2008), Wavelet-based ULF wave diagnosis of substorm expansion phase onset, *J. Geophys. Res.*, doi:10.1029/2008JA013548, in press.

Nagai, T., et al. (1998), Structure and dynamics of magnetic reconnection for substorm onsets with Geotail observations, *J. Geophys. Res.*, *103*(A3), 4419–4440, doi:10.1029/97JA02190.

Nose, M., et al. (1998), Automated detection of Pi 2 pulsations using wavelet analysis: 1. Method and an application for substorm monitoring, *Earth Planets Space*, *50*(9), 773–783.

Ohtani, S. I. (2004), Flow bursts in the plasma sheet and auroral substorm onset: Observational constraints on connection between midtail and near-Earth substorm processes, *Space Sci. Rev.*, *113*(1–2), 77–96, doi:10.1023/B:SPAC.0000042940.59358.2f.

Posch, J. L., et al. (2007), Statistical observations of spatial characteristics of Pi1B pulsations, *J. Atmos. Sol. Terr. Phys.*, *69*(15), 1775–1796, doi:10.1016/j.jastp.2007.07.015.

Roux, A., et al. (1991), Plasma sheet instability related to the westward traveling surge, *J. Geophys. Res.*, *96*(A10), 17,697–17,714, doi:10.1029/91JA01106.

Russell, C. T., et al. (2008), THEMIS ground-based magnetometers, *Space Sci. Rev.*, in press.

Sibeck, D. G., and V. Angelopoulos (2008), THEMIS science objectives and mission phases, *Space Sci. Rev.*, in press.

Voronkov, I., E. F. Donovan, B. J. Jackel, and J. C. Samson (2000), Large-scale vortex dynamics in the evening and midnight auroral zone: Observations and simulations, *J. Geophys. Res.*, *105*(A8), 18,505–18,518.

Voronkov, I. O., et al. (2003), Observations of the phases of the substorm, *J. Geophys. Res.*, *108*(A2), 1073, doi:10.1029/2002JA009314.

Yumoto, K., et al. (1990), Multiple ground-based and satellite-observations of global pi-2-magnetic pulsations, *J. Geophys. Res.*, *95*(A9), 15,175–15,184, doi:10.1029/JA095iA09p15175.

Zesta, E., L. R. Lyons, and E. Donovan (2000), The auroral signature of earthward flow bursts observed in the magnetotail, *Geophys. Res. Lett.*, *27*(20), 3241–3244, doi:10.1029/2000GL000027.

Zesta, E., L. Lyons, C.-P. Wang, E. Donovan, H. Frey, and T. Nagai (2006), Auroral poleward boundary intensifications (PBIs): Their two-dimensional structure and associated dynamics in the plasma sheet, *J. Geophys. Res.*, *111*, A05201, doi:10.1029/2004JA010640.

V. Angelopoulos and C. T. Russell, Institute of Geophysics and Planetary Physics, University of California, Los Angeles, CA 90095-1567, USA.

H. U. Frey and S. B. Mende, Space Sciences Laboratory, University of California, 7 Gauss Way, Berkeley, CA 94720-7450, USA.

A. Kale, I. R. Mann, D. K. Milling, K. R. Murphy, A. Parent, I. J. Rae, and C. E. J. Watt, Department of Physics, University of Alberta, Edmonton, AB, Canada T6G 2G7. (jrae@phys.ualberta.ca)